CrossMark

Molecular basis for the catalytic inactivity of a naturally occurring near-null variant of human ALOX15

Thomas Horn [a,*], Igor Ivanov [b], Almerinda Di Venere [c], Kumar Reddy Kakularam [d], Pallu Reddanna [d,e], Melanie L. Conrad [f], Constanze Richter [g], Patrick Scheerer [h], Hartmut Kuhn [a,*]

[a] Institute of Biochemistry, University Medicine Berlin-Charité, Charitéplatz 1, D-10117 Berlin, Germany
[b] Institute of Toxicology and Pharmacology, University of Rostock, Schillingallee 70, D-18057 Rostock, Germany
[c] Department of Experimental Medicine and Surgery, University of Tor Vergata, Via Montpellier 1, I-00133 Rome, Italy
[d] School of Life Sciences, University of Hyderabad, Hyderabad 500046, Andhra Pradesh, India
[e] National Institute of Animal Biotechnology, Hyderabad 500046, Andhra Pradesh, India
[f] Institute of Microbiology and Hygiene, University of Medicine Berlin-Charité, Hindenburgdamm 27, D-12203 Berlin, Germany
[g] Institute of Nutrition Technology and Chemistry, Technical University, Gustav-Meyer-Allee, D-13355 Berlin, Germany
[h] Institute of Medical physics and Biophysics, University Medicine Berlin-Charité, Charitéplatz 1, D-10117 Berlin, Germany

ARTICLE INFO

ABSTRACT

Mammalian lipoxygenases belong to a family of lipid-peroxidizing enzymes, which have been implicated in cardiovascular, hyperproliferative and neurodegenerative diseases. Here we report that a naturally occurring mutation in the hALOX15 gene leads to expression of a catalytically near-null enzyme variant (hGly422Glu). The inactivity may be related to severe misfolding of the enzyme protein, which was concluded from CD-spectra as well as from thermal and chemical stability assays. In silico mutagenesis experiments suggest that most mutations at hGly422 have the potential to induce sterical clash, which might be considered a reason for protein misfolding. hGly422 is conserved among ALOX5, ALOX12 and ALOX15 isoforms and corresponding hALOX12 and hALOX5 mutants also exhibited a reduced catalytic activity. Interestingly, in the hALOX5 Gly429Glu mutants the reaction specificity of arachidonic acid oxygenation was shifted from 5S- to 8S- and 12R-H(p)ETE formation. Taken together, our data indicate that the conserved glycine is of functional importance for these enzyme variants and most mutants at this position lose catalytic activity.

© 2013 Elsevier B.V. All rights reserved.

1. Introduction

Lipoxygenases (LOX) are non-heme iron containing enzymes that catalyze the dioxygenation of poly-unsaturated fatty acids containing a cis/cis 1,4-pentadiene structure to their corresponding hydroperoxides [1,2]. LOX genes occur in a few bacteria, fungi, plants and animals but are lacking in archae [3–6]. According to the positional specificity of arachidonic acid oxygenation mammalian LOXs can be classified as 5-LOX, 8-LOX, 12-LOX and 15-LOX [1,2]. The 3D-structures of various mammalian LOXs have been solved [7–10] and despite subtle structural differences the published X-ray coordinates indicate a high degree of structural similarity between the different isoforms.

Human arachidonate lipoxygenases (hALOX) have been implicated in the pathogenesis of cardio-vascular [11–14] and neurodegenerative diseases [15] but the mechanistic basis for their patho-physiological role is controversially discussed. In fact, pro- [16–19] and anti-atherogenic [20–23] activities have been reported for hALOX15 in different animal atherosclerosis models and thus, the precise role of the human enzyme in atherogenesis remains to be clarified. In an attempt to shed a light on this question, different case–control studies have been carried out in which single nucleotide polymorphisms (SNPs) in the ALOX15 gene were correlated with different read out parameters of cardio-vascular diseases such as the frequency of ischemic stroke [24], coronary artery disease [25,26] and myocardial infarction [27]. Unfortunately, the functional consequences of these mutations, especially for those localized in the 3′-UTR (rs916055) and intronic gene regions (rs7217186 + rs2619112) have not been explored in detail. Functional studies for the non-synonymous hALOX15 SNP Thr560Met (rs34210653) in exon 13 have demonstrated that this mutation may cause partial destruction of the hydrogen bonding network connecting hThr560 with active site residues [28] and these structural alterations

seem to induce partial misfolding of the enzyme (see Supporting information S1).

Because of the potential role of the ALOX15 gene for atherogenesis, we searched the NCBI dbSNP databases for other non-synonymous nucleotide exchanges in the ALOX15 gene and found two rare mutations in the triplet coding for hGly422. These nucleotide exchanges lead to two non-conservative amino acid mutations (hGly422Glu, hGly422Arg). In the 3D-structure of rabbit ALOX15, which shares a high degree of amino acid conservation with the human ortholog enzyme, rGly423 (hG422) is located in the surrounding of rIle418 and rMet419, which have previously been described as position specificity determinants for mammalian ALOX15 isoforms [29–31]. Because of this structural proximity severe functional consequences have been expected for the hGly422Glu (rs61099320) and the hGly422Arg (rs147238486) exchange.

To test this hypothesis we expressed wild-type human ALOX15 and the corresponding enzyme mutants in *Escherichia coli* and characterized the purified enzymes. We found that the hGly422Glu exchange leads to a loss of catalytic activity, and more detailed structural data (CD, fluorescence measurements) show that the mutation seems to cause a change in the secondary structure composition of the protein. In contrast, the hGly422Arg mutant retained its catalytic activity and its structure is minorly affected.

2. Material and methods

2.1. Materials

The chemicals were obtained from the following sources: arachidonic acid (5Z,8Z,11Z,14Z-eicosatetraenoic acid), linoleic acid (9Z,12Z-octadeca-9,12-dienoic acid) and chloramphenicol from Sigma Aldrich (Hamburg, Germany), HPLC standards of 5($\pm$)-HETE, 8($\pm$)-HETE, 11($\pm$)-HETE, 12($\pm$)-HETE, 13($\pm$)-HODE, and 15($\pm$)-HETE from Cayman Chem. (distributed by Spi Bio, Montigny le Bretonneux, France), sodium borohydride, ampicillin from Life Technologies, Inc. (Eggenstein, Germany), kanamycin and isopropyl-β-thiogalactopyranoside (IPTG) from Carl Roth GmbH (Karlsruhe, Germany). HPLC solvents were ordered from Baker (Deventer, Netherlands) or VWR International GmbH (Darmstadt, Germany). Restriction enzymes were purchased from Fermentas (St. Leon-Rot, Germany). Oligonucleotide synthesis was performed at BioTez (Berlin, Germany) and DNA sequencing was carried out at Eurofins MWG Operon (Ebersberg, Germany). The *E. coli* strain XL-1 blue was purchased from Stratagene (La Jolla, CA), the *E. coli* strain BL21(DE3)pLysS and the fluorescent dye SYPRO Orange® were purchased from Invitrogen (Carlsbad, California, USA). The EnBase fed batch system was obtained from Biosilta (Berlin, Germany).

2.2. Methods

2.2.1. Recombinant expression and purification of hALOX, hALOX5, hALOX12 and rabbit ALOX15

In order to express hALOX15 as a His-tag fusion protein, the coding region of the corresponding cDNA was first amplified by RT-PCR and then cloned into the pET28b expression vector between the *SalI* (N-terminus) and *HindIII* (C-terminus) restriction sites. For each mutant preparation a 0.5 l fed batch liquid culture (EnBase, Biosilta) of *E. coli* BL12(DE3)pLysS was grown overnight at 30 °C until an OD_{600} ~ 15. Expression of the recombinant protein was induced by addition of 1 mM IPTG (final concentration) and the culture was kept for 24 h at 23 °C until a final OD_{600} ~ 25–30. After cultivation bacterial cells were centrifuged (3600 ×*g*, 4 °C, 10 min) and resuspended in 45 ml phosphate buffered saline (PBS). Cells were lysed by sonification, the cell debris was removed by centrifugation (23,000 ×*g*, 4 °C 45 min), and the lysis supernatant was loaded onto a 2 ml Ni-NTA agarose affinity column. To remove loosely bound proteins the column was washed

with 100 mM Tris/Cl, 300 mM NaCl (pH 8.0) with either 10 or 25 mM imidazole. The *His*-tagged fusion protein was eluted with 100 mM Tris/Cl, 300 mM NaCl, 200 mM imidazole (pH 8.0). The elution fractions were desalted and further purified by an anion exchange chromatography with a ResourceQ column (6 ml) to >95% purity (see Supporting information S2.). The purified enzyme was stored in 20 mM Tris/Cl, 150 mM sodium chloride in the presence of 10% (v/v) glycerol (pH 8.0) at −80 °C until usage.

Iron content was measured by atom absorbance spectroscopy on a PerkinElmer Life Sciences AA800 instrument equipped with an AS800 auto sampler. The iron content was related to LOX protein that was quantified spectrophotometrically (1 mg/ml pure human ALOX has an absorbance of 1.6 at 280 nm).

The expression of hALOX12, hALOX5 and rabbit ALOX15 variants was performed as previously described [32–34].

2.2.2. Lipoxygenase activity assays

ALOX activity of purified hALOX15 enzyme preparations was assayed by RP-HPLC quantification of arachidonic acid (AA) oxygenation. Purified enzyme (4 μg) was incubated with 100 μM arachidonic acid for 15 min at 37 °C. The hydroperoxide fatty acids were reduced to its equivalent hydroxides using sodium borohydride and acidified with acetic acid to pH 3. Then 500 μl of ice-cold methanol was added. The protein precipitate was centrifuged (23,000 ×*g*, 8 °C, 10 min) and aliquots of the clear supernatant were injected to RP-HPLC. Steady-state kinetic measurements were performed using a UV-2102 UV/VIS Scanning Spectrophotometer (Shimadzu, Japan). When linoleic acid was used as a substrate 1.6 μg of purified enzyme was incubated with different concentrations of this fatty acid (1–100 μM) in 1 ml PBS and the formation of conjugated dienes was followed at 235 nm over 60 s.

The activity assays for hALOX12, hALOX5 and rabbit ALOX15 variants were carried out as previously described [32–34].

2.2.3. HPLC analysis

HPLC of the LOX products was performed on a Shimadzu LC-20 instrument equipped with an auto sampler by recording the absorbance at 235 nm. Reverse phase-HPLC was carried out on a Nucleodur C18 Gravity column (Macherey-Nagel, Düren, Germany; 250 × 4 mm, 5 μm particle size) coupled with a guard column (8 × 4 mm, 5-μm particle size). A solvent system of methanol/water/acetic acid (85/15/0.05, by vol.) was used at a flow rate of 1 ml/min. Straight phase-HPLC (SP-HPLC) was performed on a Nucleosil 100-5 column (250 × 4 mm, 5 μm particle size) with the solvent system n-hexan/2-propanol/acetic acid (100/2/0.1, by vol.) and a flow rate of 1 ml/min. Enantiomers of hydroxylated fatty acid were separated by chiral phase HPLC (CP-HPLC) employing different types of Chiralcel (Daicel Chem. Ind., Ltd.) columns. As mobile phase a mixture of n-hexane/2-propanol/acetic acid at a flow rate of 1 ml/min was used, in which the 2-propanol content was varied for the different positional isomers: 15-HETE: Chiralcel OD column, 5% 2-propanol; 5-HETE: Chiralcel OB column, 4% 2-propanol. 8 and 12-HETE were additionally separated by a solid-phase HPLC and then methylated with diazomethane. Enantiomers of 8-HETE-methylester were separated on a Chiralcel OB column with a solvent system n-hexane/2-propanol/acetic acid (100/4/0.1, by vol.) and 12-HETE-methylester enantiomers were separated on a Chiralcel OD column with a solvent system (100/2/0.1, by vol.).

2.2.4. Thermal shift assay (thermal denaturation)

Purified LOX enzyme (3 μM) was incubated with a 2.5 fold molar excess of fluorescent SyproOrange® dye in 20 mM Tris/Cl 150 mM NaCl (pH 8.0), total volume 20 μl. The heat denaturation reaction was performed on a Rotor-Gene RG-3000 real-time PCR machine (Corbett Research) heating up the probes from 30 to 95 °C at a rate of 0.5 °C/s. The fluorescent dye SyproOrange® is normally quenched in aqueous solutions. Thermal unfolding of the protein leads to the exposition of hydrophobic core regions to the surface, where the dye can bind and
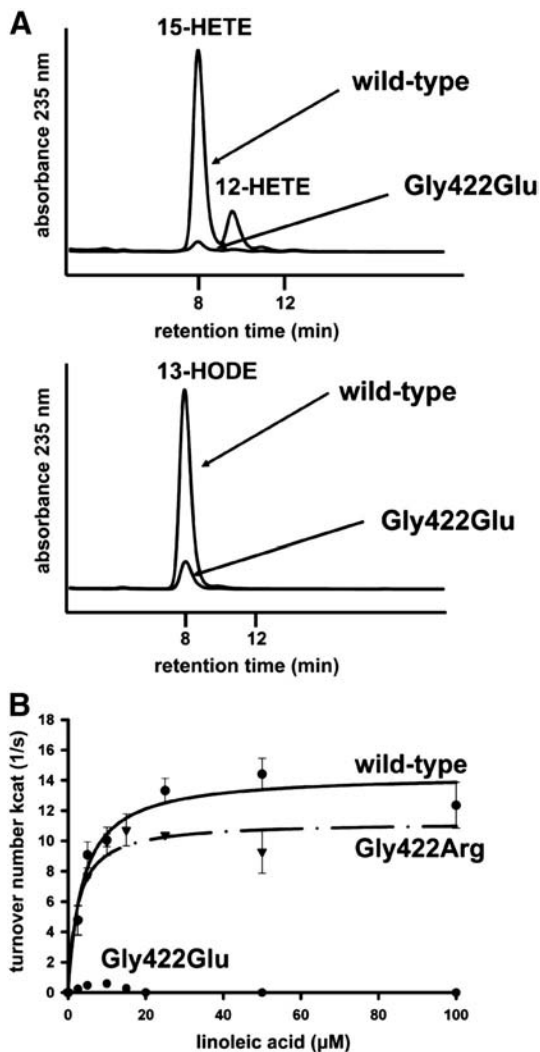
Fig. 1. Protein chemical end enzymatic characterization of human ALOX15 variants. (*A*) *Reverse-phase HPLC chromatogram of hALOX15 wild-type and hGly422Glu.* The RP-HPLC chromatogram shows that the wild-type has a major 15- and a minor 12-arachidonate oxygenation specificity and an exclusive 13-linoleate oxygenation specificity, which is typical for this LOX isoform; the hGly422Glu variant is nearly inactive and has an atypical reaction spectra. (*B*) *Michaelis–Menten kinetics of hALOX15 and hGly422Glu + hGly422Arg mutant.* The kinetic measurements with linoleic acid (LA) as a substrate show that the wild-type enzyme and the hGly422Arg mutant follow Michaelis–Menten and are therefore fitted with a hyperbolic equation whereas the hGly422Glu mutant is a nearly inactive enzyme variant.

becomes unquenched causing a fluorescent increase. The resulting fluorescence was detected using a FAM/SYBR green filter. The software Rotor-Gene 4.6 was used for calculation of the negative first derivative of the raw data. The inflection point of the melting transition is the melting point (T_m). Figures were generated with SigmaPlot. The melting point for each mutant was analyzed in 3–4 independent experiments.

2.2.5. Circular dichroism (CD) and fluorescence spectroscopy

The CD, steady-state fluorescence measurements and GdHCl denaturation studies were performed as previously described [34]. Briefly, circular dichroism measurements were performed using a Jasco-710 spectropolarimeter. Spectra were collected in the peptidic region with a 0.1 path length quarts cell at different temperatures (protein concentration 0.13 mg/ml in 20 mM Tris/Cl buffer at pH 8.0). Steady-state fluorescence measurements were recorded with an ISS-K2 fluorometer (ISS, Champaign, IL, USA) upon excitation at 280 nm (protein concentration 0.13 mg/ml in 20 mM Tris/Cl, pH 8.0). The aliquots of the denaturant stock solutions (8 M GdHCl in 20 mM Tris/Cl buffer at pH 8.0) were used to prepare a series of solutions. The mean residue ellipticities of the different solutions were measured by CD at 220 nm and static fluorescence emission spectra at 20 °C. Each measurement was repeated at least three times, and the relative standard deviation was reported in the figures as an error bar. The reversibility of the process was checked obtaining protein refolding by diluting a highly concentrated unfolded protein sample in 20 mM Tris/Cl buffer at pH 8.0. A three-state model in which existence of monomeric intermediate protein species is supposed to be in equilibrium with both the native and unfolded protein molecules was used to fit the fluorescence and CD data.

2.2.6. Immunoblotting

To quantify the relative amounts of different hALOX12 and hALOX5 variants in different enzyme preparations, immunoblotting was carried out as previously described [32,33].

2.2.7. Structural analysis, in silico mutagenesis, homology modeling and amino acid alignment

2.2.7.1. Structural analysis of rabbit ALOX15 and in silico mutagenesis.
The crystal structure of the rabbit ALOX15 (PDB: 2P0M) was used as the structural model for our hypothesis. Rabbit ALOX15 shares an 80% amino acid homology with its human homologue and represents therefore a useful model for our study. *In silico* mutations in rabbit ALOX15 structure was performed on Maestro 9.3 (Schrödinger, LLC, New York, USA, 2012) and all mutants were further minimized by 5000 steps of SD and 10,000 steps of PRCG methods with 0.05 gradient. This protein structure minimization protocol was done using MacroModel 9.9 (Schrodinger, LLC, New York, 2012). Visualization and analysis of the results were done using PyMol (Schrodinger, New York, USA) and Accelrys discovery Studio 3.1. (Accelrys, San Diego, USA).

2.2.7.2. Homology modeling and structural analysis of human ALOX15.
Homology modeling of human ALOX15 was done by taking the protein sequence from NCBI (GenBank ID: AAA36182.1) and using rabbit ALOX15 (PDB ID: 2P0M) as structural template. The software Prime 3.1 (Schrödinger, LLC, New York, 2012) was used to build the structure model. Further, non-template loops are refined and the protein is relaxed by minimizing with 5000 steps of SD and 10,000 steps of

Table 1
Kinetic characterization of naturally occurring hALOX15 variants.
Purified recombinant hALOX15 wild-type and the natural occurring hGly422 mutants were incubated with arachidonic and linoleic acid (n = 4). The amounts for 15-HETE formation were quantified for each sample, and wild-type 15-HETE formation was set to 100%. The k_{cat} and K_m values of the hALOX15 variants for linoleic acid were taken from the hyperbolic equations of the Michaelis–Menten kinetics. The hGly422Glu mutant does not follow the Michaelis–Menten principle and therefore a determination of kinetic parameters with a hyperbolic equation is not possible.

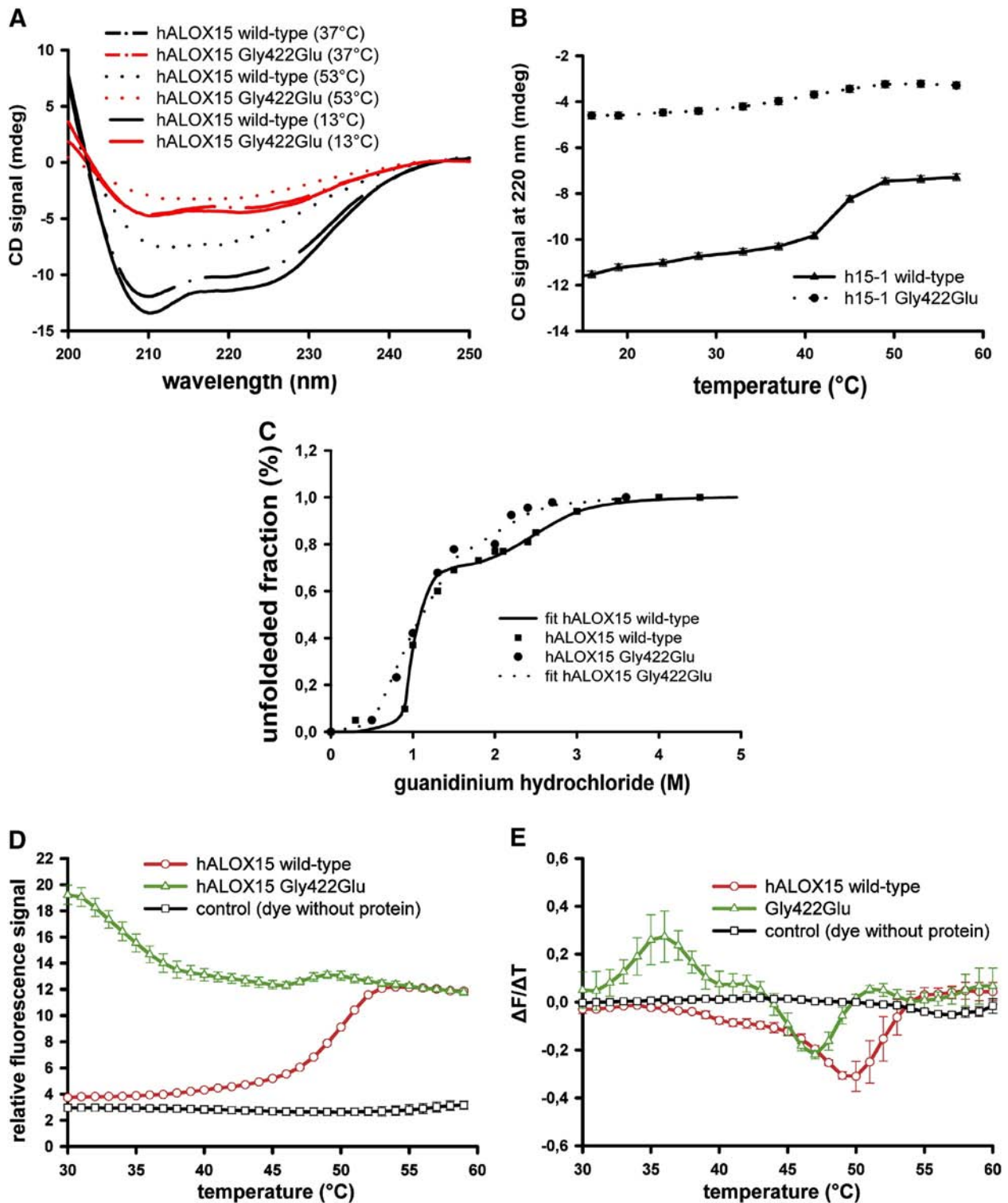| hALOX15	Share of 15-HETE %	Rel. activity (AA) %	k_{cat}(LA) s^{-1}	K_m(LA) µM	R^2
Wild-type	83 ± 4	100 ± 1	14.4 ± 0.8	3.8 ± 1.0	0.89
Gly422Glu	83 ± 4	<1	n.d	n.d	n.d.
Gly422Arg	89 ± 7	36 ± 3	9.6 ± 0.7	1.7 ± 0.8	0.96

Fig. 2. Thermodynamic characterization of human ALOX15 variants. (*A*) *Comparison of CD spectra of hALOX15 wild-type and its hGly422Glu mutant at different temperatures.* The CD spectra at different temperatures (13, 37 and 53 °C) reveal that there are major differences between the wild-type enzyme and its mutant in the secondary and tertiary structure composition. Inactivity seems to be caused by a misfolding of the hGly422Glu mutant. (*B*) *Thermostability of hALOX15 wild-type and hGly422Glu.* The figure shows the dependence of the CD signal at 220 nm from the increasing temperature. The heat denaturation behavior of the mutant strongly differs from the wild-type enzyme. (*C*) *Unfolding profile of hALOX15 LOX and hGly422Glu mutants as a function of chemical denaturant (GdHCl).* The unfolded fraction was monitored through both fluorescence steady state spectroscopy and circular dichroism and the fraction of unfolded molecules were plotted *vs.* the GdHCl concentration. Occasionally the fit of unfolding curves followed by fluorescence and CD could be described using single equation suggesting that both secondary and tertiary structure follow similar unfolding kinetics. The existence of a plateau in the range 1.8–2.6 M GdHCl concentrations suggested that unfolding pathway may be described with a 3-state model N $\leftarrow \rightarrow$ I $\leftarrow \rightarrow$ U where N is the native state, I is a partially folded state and U is the completely unfolded protein. The line is the fit of the unfolding process and the points represent single measurements (position of the fluorescence spectrum and CD intensity at 222 nm). (*D and E*) *Thermostability of hALOX15 wild-type and the hGly422Glu mutant using a fluorescent-based thermodynamic shift assay.* The figure shows the dependence of tertiary structure from the increasing temperature. SYPRO Orange® is a fluorescent dye, which is quenched in aqueous solutions. As temperature rises, protein undergoes thermal unfolding and hydrophobic core regions are exposed to the surface. SYPRO Orange® then binds to these regions and becomes unquenched. With increasing temperature, the amount of denaturized protein is increased causing an increase of the fluorescence signal. The thermal denaturation curve (Fig. 2D) of the hGly422Glu (green) mutant strongly differs from the wild-type enzyme (red) indicating that is has a differential folding. The negative first derivative (panel E) is calculated to determine the inflection point of the unfolding curve more accurately. The wild-type enzyme has a melting temperature (T_m) of 50 °C.

Table 2
Thermodynamic unfolding parameters of hALOX15 wild-type and hGly422Glu mutant.

hALOX15	I transition		II transition	
	ΔG_1 (kcal/mol)	m_1 (kcal $*$ mol^{-1} $*$ M^{-1})[a]	ΔG_2 (kcal/mol)	m_2 (kcal $*$ mol^{-1} $*$ M^{-1})[a]
Wild-type	10.5	10.0	4.0	1.6
Gly422Glu	4.0	3.9	3.5	1.8

[a] Slopes of the free energy plots in Fig. 2D in kcal $*$ mol^{-1} $*$ M^{-1}.

PRCG methods with 0.05 gradient. The energetically minimized human ALOX15 model was used to understand the structural changes of the Gly423Glu mutant (see Supporting information S2). Same methodology employed for analyzing the mutants of rabbit ALOX15 was used as mentioned above.

2.2.7.3. Structural analysis of human ALOX15B. A protein model from the Protein model database (PMDB) was used for structural analysis of human ALOX15B (PMDB code: PM0078035). The software PyMol (Schrödinger, LLC, New York, USA) was used for visualization and structural analysis.

2.2.7.4. Sequence alignment and genetic variants. Multiple sequence alignment was performed with the Clustalw2 program (European Bioinformatics Institute, Cambridge, UK) setting default parameters. ALOX sequences and the information related to the naturally occurring hALOX15 variants (Gly422Glu, Gly422Arg) were extracted either from the NCBI dbSNP database (National Center for Biotechnology Information, Bethesda, USA) or 1000 genome project (www.1000genomes.org).

3. Results

3.1. The hGly422Glu mutant is a naturally occurring near-null variant of human ALOX15

To explore the catalytic properties of the hALOX15 variants, which are encoded by the naturally occurring SNPs, wild-type hALOX15 together with the hGly422Glu and hGly422Arg mutants were expressed in *E. coli* and purified to apparent electrophoretic homogeneity (see

Fig. 3. Structural characterization of rabbit ALOX15. *rGly423 forms a main-chain-side-chain interaction with an aspartate residue close at the active site* The figure shows the structure of the rabbit ALOX15 (PDB: 2P0M). The N-terminal β-barrel domain is colored in yellow, while the catalytic domain is shown as marine cartoon. The previous described position specifity determinants (rPhe353, rIle418 and rIle593), also known as "triad", are represented as orange spheres. The rGly423 residue interacts with rAsp416 (black dashes) close to one of the triad determinants (rIle418) close to the active site. The distance between the carboxylic group and glycine amide group is 2.6 Å, which is in range of a hydrogen bond.

Supporting information S4). Aliquots of the purified enzyme preparations were subsequently incubated with arachidonic acid or linoleic acid, and the reaction products were analyzed by RP-HPLC. As expected 15-H(p)ETE and 13-H(p)ODE were the dominant reaction products of the wild-type enzyme (Fig. 1A) and a similar product pattern was analyzed for the hGly422Arg mutant. The hGly422Glu variant did not produce any oxygenation products since the small peaks comigrating with the authentic HETE-standards were the products of the substrate autoxidation. For a more detailed characterization of the kinetic properties of the mutant enzyme species, continuous spectrophotometric measurements were carried out (Fig. 1B): the basic kinetic constants are summarized in Table 1. Taken together the data indicate that the hGly422Glu mutant was catalytically silent with both, linoleic acid and arachidonic acid. In contrast, the hGly422Arg variant exhibited a residual arachidonic and linoleic acid oxygenase activity of 40–70%. V_{max} (k_{cat}) and K_M values determined with linoleic acid for the wild-type enzyme and its hGly422Arg variant (Table 1) are comparable with the data reported for the wild-type enzyme (Brenda Enzyme databank ALOX15 EC 1.13.11.33, k_{cat}: 4–17.8 s^{-1} K_M: 3–9.5 µM).

LOX enzymes contain equimolar amounts of non-heme iron, which is essential for the catalytic activity [35]. To explore the possible reasons for the catalytic silence of the hGly422Glu mutant, we quantified the iron content of our enzyme preparations and found an apoprotein to iron ratio of approximately 0.8 for all enzyme preparations.

3.2. Gly422Glu mutation induces structural changes of the hALOX15

Since a lack of catalytic iron was not responsible for inactivity of the hGly422Glu mutant, we compared other structural properties of wild-type hALOX15 and the mutant enzyme (Fig. 2). Comparison of the CD-spectra at native conditions (13 and 37 °C) and those of partly denatured protein (53 °C) indicated drastic differences between wild-type and the mutant enzyme (Fig. 2A). The thermal denaturation curve of the wild-type enzyme (Fig. 2B) follows a two-state transition model with a melting point (T_m) of ~45–46 °C. As for the hGly422Glu mutant, its secondary structure was strongly disordered even at low temperature suggesting strong impact of the mutation on the structural performance of the mutant protein. To further study intrinsic properties of both proteins enzyme unfolding was monitored at increasing concentrations of guanidine hydrochloride (GdHCl), which binds to peptide bonds and the alterations either in the CD spectra of fluorescence emission signal were recorded (Fig. 2C). On the basis of the raw experimental data we performed three-state transition calculations common for LOX proteins [34,36]. The results are summarized in Table 2. The first transition of the Gly422Glu mutant requires 2.5 times less energy than that of the wild-type enzyme ($\Delta\Delta G_1$ ~ 6 kcal/mol), and is accompanied with the smaller change in the accessible surface area (ΔASA) upon its denaturation (m-values) [37]. Alternatively, we performed thermostability assays employing an external fluorescent dye which preferentially binds to the hydrophobic core residues during the denaturation of proteins and thus, an increase in the fluorescence intensity indicates a higher exposition of hydrophobic residues to the surface. The thermal denaturation of the wild-type enzyme follows a two-state transition N ← → U, where N is the native state (30 °C) and U the unfolded state (plateau at 50–60 °C) (Fig. 2D). The inflection point of the first negative derivative of the denaturation curve (Fig. 2E) leads to a
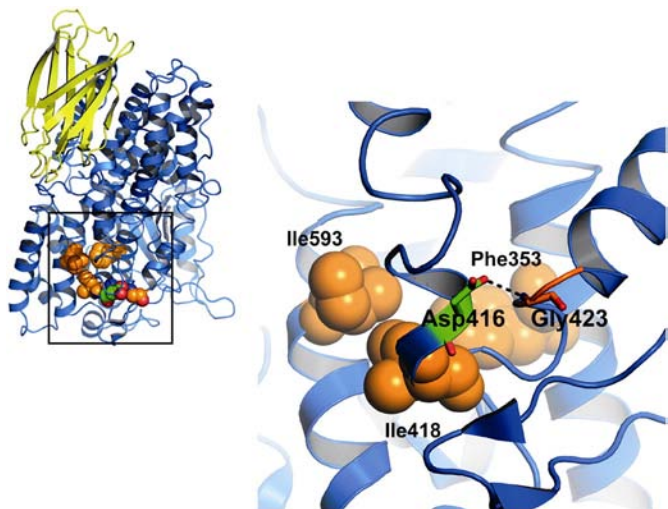
melting point (T_m) for the wild-type enzyme of 50 °C, which is consistent with the value determined by the CD measurements. Comparison of the denaturation curves of the wild-type and the Gly422Glu shows that the mutant variant (Fig. 2D) at lower temperature (30 °C) exhibits a similar binding affinity to the fluorescence dye as the wild-type enzyme does at 55 °C. Taken together, these data indicate that the inactivity of the Gly422Glu mutant might be caused by a differential folding of the enzyme with an increased exposure of hydrophobic core residues to the solvent.

3.3. Different mutations of hGly422 cause a loss in enzymatic activity and induce structural changes

As indicated above the natural occurring hGly422Glu mutant is an inactive and differentially folded hALOX15 variant. In the crystal structure of the rabbit ALOX15 (PDB: 2P0M) Gly423 (hG422) is located in a loop region that interconnects two α-helices. One of these helices carries rIle418, which contributes to the bottom of the U-shaped substrate binding pocket (Fig. 3). Mutations of this residue alter the positional specificity and catalytic activity of various mammalian ALOX15 isoforms [29–33]. In the crystal structure of rabbit ALOX15 the glycine residue 423 (hG422) stabilizes the active site by forming a main-chain-side-chain hydrogen bond with rAsp416 (hAsp415) (Fig. 3). In fact, the distance between the carboxylic group of the aspartate and the amide group of the glycin is 2.6 Å, which is a suitable hydrogen bonding distance [38].

In the ALOX15 structure rGly423 interacts with rAsp416 via a main-chain–side-chain interaction, which might be interrupted by the Gly-to-Glu exchange. The amide moiety of the glycine residue is not expected to be altered by the mutation but introduction of the negatively charged side chain of glutamate at the 422 position may lead to structural alterations causing protein misfolding and loss of catalytic activity (Fig. 4C). To explore whether the charge or the size of the naturally occurring hGly422Glu and hGly422Arg mutations might be the reason for the enzyme functional and structural distortion we introduced an uncharged residue with similar space-
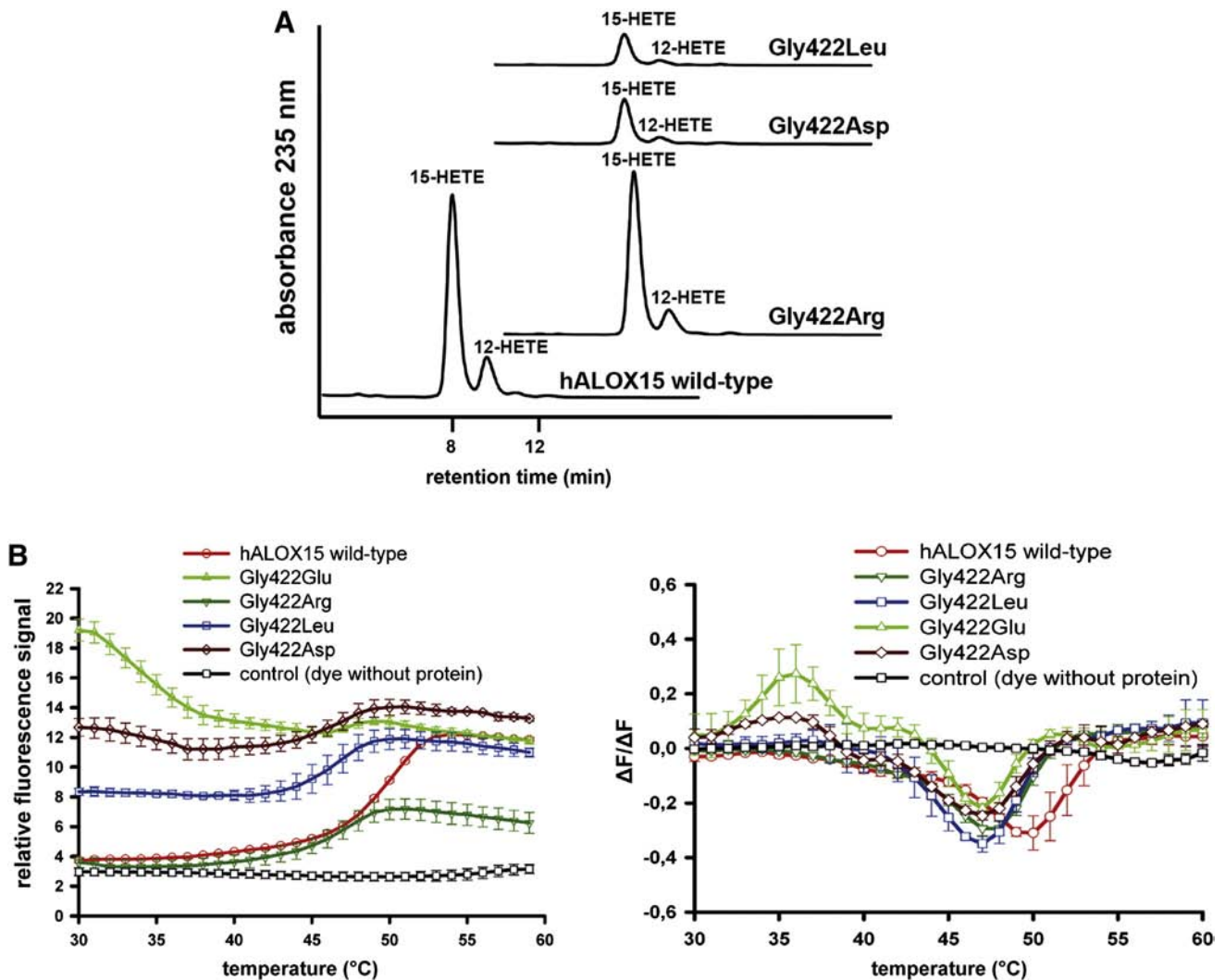

Fig. 4. Structural and functional characterization of human ALOX15 mutants at Gly422. (*A*) *Positional specificity of hALOX15 Gly422 mutants.* The RP-HPLC spectra of different mutations after incubation with arachidonic acid show that none of analyzed mutations has an effect on the product specificity of hALOX15 enzyme. All mutations at hGly422 cause a reduction of enzymatic activity resulting in a decreased 15-HETE HPLC signal. (*B*) *Thermal shift assay of different hALOX15 Gly422 mutations.* Thermal shift assay reveals that the mutations hGly422Glu, hGly422Asp and hGly422Leu have an increased fluorescence signal at room temperature which indicates differences in the secondary/tertiary structure composition in comparison to the wild-type enzyme. In contrast to this, the hGly422Arg variant starts at a similar level as the wild-type, this indicates that the mutation has only minor effects on the enzyme structure. The negative first derivatives show that all mutants seem to destabilize the protein because they all have a decreased melting temperature in comparison to the wild-type enzyme. (*C*) *Structural explanation for different effects of hALOX15 Gly422 mutants.* To explain the molecular effects of different mutants at the rGly423 position the residue was mutated *in silico* in the rabbit ALOX15 structure (PDB: 2P0M) and energetically minimized (see Material and Methods). The representation is the similar like described in Fig. 3. The mutated residues are shown as white sticks and the resulting sterical clash which is caused by some mutations is shown as red dots. One can see that all mutations at the rGly423 position cause a strong sterical clash in the surrounding which might be the reason for the misfolding and inactivity of these enzyme variants.
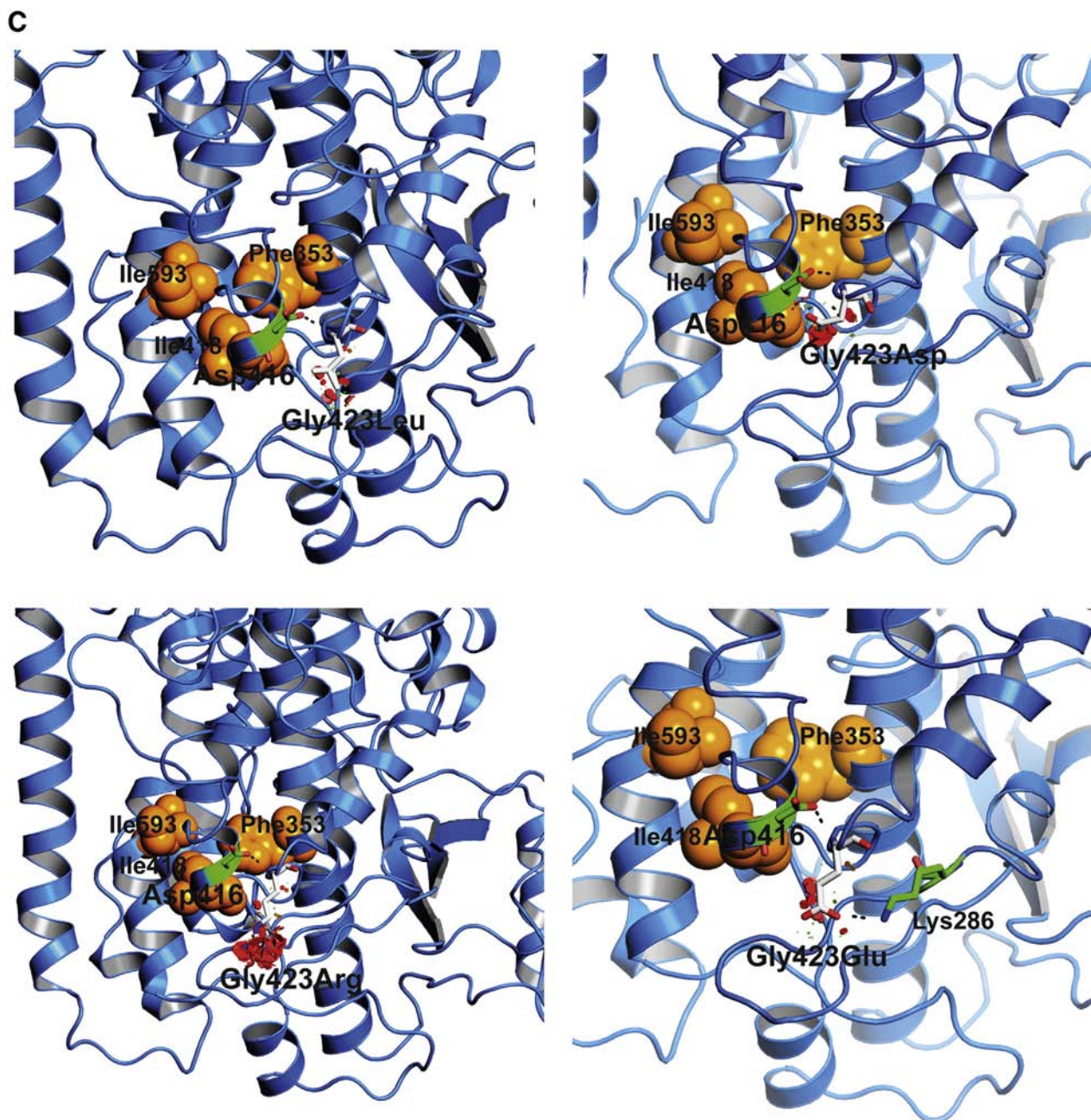
Fig. 4 (*continued*).

requiring properties (Leu) and a potentially negative charged residue (Asp) at this position. Both mutants (hGly422Leu and hGly422Asp) exhibit a strongly reduced catalytic activity (Table 3), and exhibit a
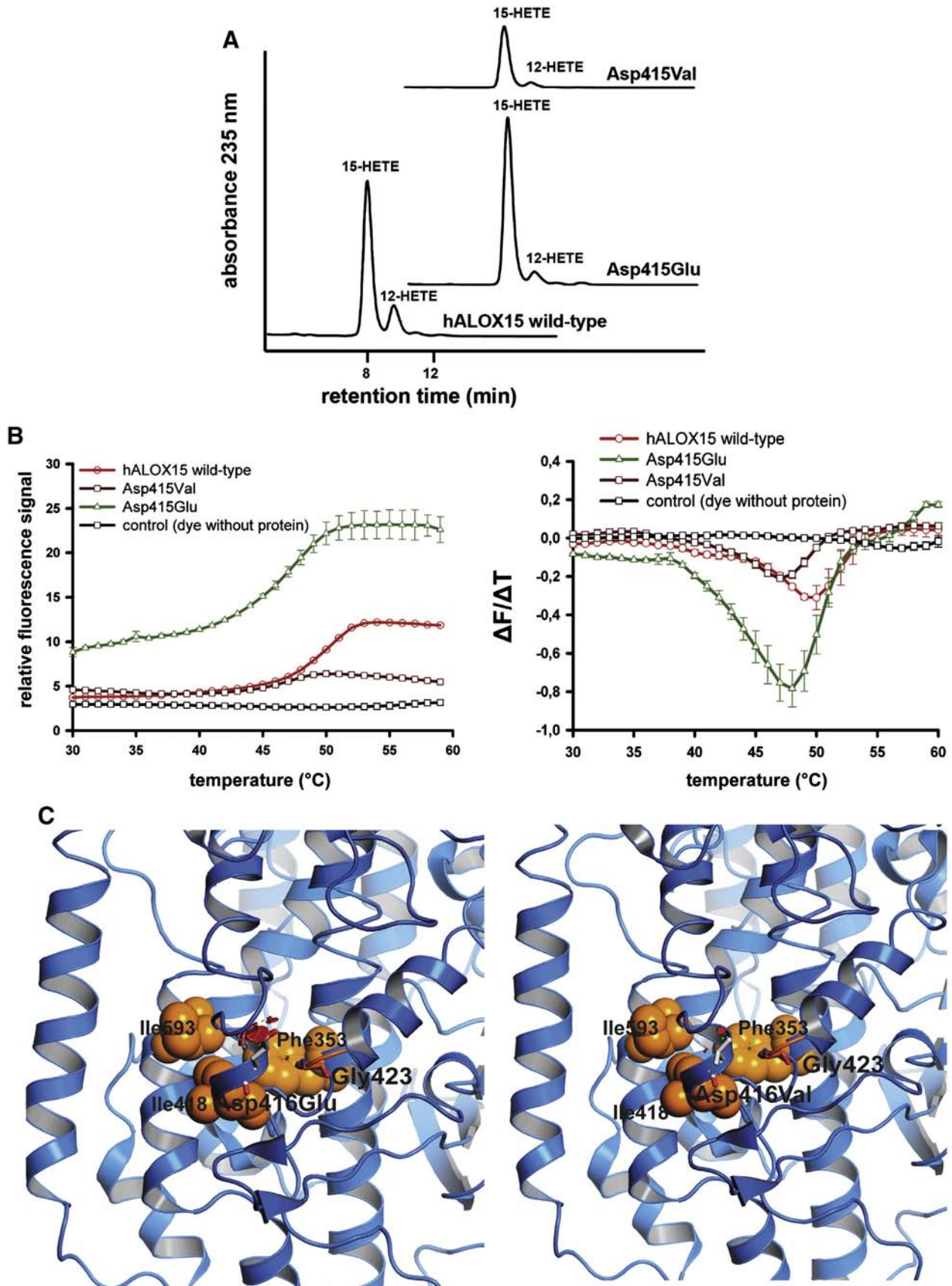
higher affinity to the fluorescence dye indicating that the overall structure of the enzyme has been altered (Fig. 4B). When we compared the degree of structural differences between wild-type hALOX15, its

Table 3
Comparison of relative catalytic activities and melting points of different hALOX15 variants.

Purified recombinant hALOX15 wild-type and the hGly422 and hAsp415 mutants were incubated with arachidonic acid (n = 4). The amounts for 15-HETE were quantified for each sample, and wild-type 15-HETE formation was set to 100%. Thermal shift assays (n = 3–4) were performed, with the inflection point of the first negative derivative representing the melting point of the enzyme variant. The temperature difference ΔT between the melting points of wild-type and mutant was calculated as follows: T_m (mutant) $- T_m$ (wild-type). All mutants have an approximate 2–3 °C decreased melting temperature in comparison to the wild-type which indicates that they destabilize the protein.

hALOX15	Share of 15-HETE %	Rel. activity (AA) %	Melting point T_m (°C)	ΔT (°C)
Wild-type	83 ± 4	100 ± 1	50.0 ± 0.6	0
Gly422Glu	83 ± 4	<1	n.d.	n.d.
Gly422Arg	89 ± 7	36 ± 3	47.8 ± 0.3	−2.2
Gly422Leu	87 ± 1	14 ± 1	47.4 ± 0.4	−2.6
Gly422Asp	91 ± 1	18 ± 1	47.1 ± 0.1	−2.9
Asp415Glu	91 ± 1	97 ± 1	47.2 ± 0.3	−2.8
Asp415Val	91 ± 1	34 ± 5	47.5 ± 0.5	−2.5

hGly422Glu, hGly422Asp and hGly422Leu mutants we found that the alterations induced by incorporation of the two negatively charged residues are somewhat stronger since the fluorescence signal is higher

at 30 °C. In turn, the fluorescence signal of the hGly422Arg mutant is similar to that of the wild-type enzyme (Fig. 4B) indicating that enzyme structure is not as strongly affected by the mutation. Except for

hGly422Glu, whose thermal denaturation does not follow a two-state transition (Fig. 4B), melting temperatures (T$_m$) of other hGly422 variants (Gly422Asp, Gly422Arg, Gly422Leu) are ~2–3 °C lower than that of the wild-type enzyme indicating that all mutations are destabilizing the entire enzyme, which might be a plausible reason for the reduced catalytic activity (14–36% residual catalytic activity for arachidonic acid, Table 3). Indeed, *in silico* mutagenesis studies suggest that all mutations at hGly422 cause steric clash with the side-chains of surrounding residues (Fig. 4C).

3.4. Effects of mutations at the interaction partner hAsp415 are less pronounced

To explore the functional role of the hydrogen bond between hAsp415 and hGly422 for structural integrity of hALOX15, we introduced an either hydrophobic (Val) or other polar (Glu) residue at this position. Although hAsp415Val mutation does not have major effects on the structure of the enzyme as suggested by *in silico* mutagenesis studies (Fig. 5C) and the thermal melting temperature of hAsp415Val mutant was obtained to be 2.5 °C lower than the corresponding value of the wild-type enzyme (Fig. 5B), its arachidonate oxygenation activity was reduced by 60% (Table 3). In contrast, for the hAsp415Glu mutant we only observed minor functional differences (Table 3). At room temperature, however, the fluorescence signal for the hAsp415Glu mutant was higher than that for the wild-type enzyme suggesting partial misfolding of the mutant protein (Fig. 5B). To explain this data one may assume that the larger glutamate side chain clashes with other side chains to induce subtle structural alterations (Fig. 5C). Compared with the wild-type enzyme, the T$_m$ value for the hAsp415Glu mutant was reduced by 2.8 °C (Fig. 5B + Table 3) suggesting that this mutation also gradually destabilized the enzyme structure. However, the degree of structural alterations should have been rather small since only minor impact on its catalytic activity was observed. Summarizing, both mutations result in a partial destabilization of the enzyme structure but are not sufficient to induce a loss of enzyme function.

3.5. Is the conserved glycine residue also important in other mammalian lipoxygenases ?

Multiple sequence alignments of mammalian LOX isoforms (Fig. 6) indicated the conservation of the glycine residue among ALOX5, ALOX12, and ALOX15 isoforms of different species, whereas in the epidermal lipoxygenases (ALOX15B, ALOX12B, and ALOXE3) this residue is not conserved. In the 3D-structure of hALOX5 a hydrogen bond is formed between the Asp422 and Gly429 (corresponding residues in hALOX15 D415 and G422) whereas in the porcine ALOX12 Asp416 and Gly423 interact. Based on our mutagenesis data obtained for hALOX15 we predicted that a similar mutagenesis strategy for hALOX5 and hALOX12 may lead to inactive enzyme species, created the corresponding Gly-to-Glu mutants of hALOX12 and hALOX5 and assayed the catalytic activity and the product specificity of the enzyme. The results summarized in Table 4 indicated that the Gly422Glu exchange causes a 70% loss in arachidonic acid oxygenase activity in hALOX12, whereby the reaction specificity of the enzyme was not altered. For hALOX5, a similar mutagenesis strategy induced a 50% loss in arachidonate oxygenase activity (Table 4) associated with significant alterations in the reaction specificity since this mutant was predominantly 8S- and 12R-HpETE producing enzyme (data not shown).

This data suggest that this glycine residue, which is conserved in several human LOX isoforms, appears to be important for the catalytic activity and the structural performance of ALOX proteins.

4. Discussion

4.1. Gly422Glu and Gly422Arg are rare natural occurring hALOX15 variants

Human ALOX15 and different genetic variants have been implicated in the pathogenesis of atherosclerosis [16–19,25–27], and the enzyme is discussed to play a key role in the biosynthesis of atheroprotective eicosanoids such as resolvins and lipoxins [22,23]. A loss-of-function mutation in at least one hALOX15 allele seems to increase the risk of coronary artery disease [26], which might be caused by a reduced formation of anti-inflammatory and atheroprotective resolvins and lipoxins. For this reason, similar biological effects should be expected for other inactive hALOX15 variants. In our study we analyzed the molecular basis for the reduced catalytic activity of two rare naturally occurring hALOX15 mutants at position 422. The hGly422Glu variant was an inactive and differentially folded enzyme species. The hGly422Arg mutant also exhibited a decreased thermostability, which might be the reason for its reduced catalytic activity, but its tertiary structure was barely affected.

The hGly422Arg variant is a rare enzyme variant, which occurs with a global allele frequency of <1% (NCBI dbSNP database, Minor allele frequency MAF T = 0.001, Minor allele count MAC = 1), whereas neither in the NCBI nor 1000 genome SNP databases any frequency data is available for the hGly422Glu mutant [39]. Since homozygous allele carriers of the hGly422Glu exchange constitute functional hALOX15 knockouts and since no global frequency data for this SNP are available, we analyzed the distribution of this enzyme variant in 306 German healthy volunteers. Unfortunately, none of the individuals carried the minor mutant allele suggesting an allele frequency of <0.3%. Thus, it must be classified as a rare enzyme variant. Our findings are consistent with a major conclusion of the 1000 genome project suggesting that usually damaging and pathological-associated genetic variants have a rare distribution with a global frequency < 0.5% [39].

4.2. hGly422–hAsp415 interaction is important for enzyme functionality

The Gly422–Asp415 interaction in human ALOX15 might be disturbed by introducing space-filling side-chain residues or by other mutations at the hGly422, which showed a reduced catalytic activity and were partially misfolded. In contrast, mutations at hAsp415 cause only minor functional defects. Nevertheless the hAsp415Val mutation reduces the catalytic activity and thermostability, which indicates that the polar hGly422–hAsp415-interaction has a stabilizing function on the enzyme, although its loss might not be the primary reason for the partial protein misfolding.

In the crystal structure of the rabbit ALOX15 (80% sequence homology with human enzyme) rGly423 is not an immediate active site residue but it is in close proximity to rIle418 and rMet419 [30,31], two active

Fig. 5. Structural and functional characterization of human ALOX15 mutants at Asp415. (*A*) *Activity of hALOX15 Asp415 mutants*. The RP-HPLC spectra of different mutations after incubation with arachidonic acid show that none of analyzed mutations has an effect on the product specificity of hALOX15 enzyme. Only the hAsp415Val mutant shows a reduced enzymatic activity, whereas the hAsp415Glu mutant reveals a similar activity like the wild-type enzyme. (*B*) *Thermal shift assay of different hALOX15 Asp415 mutations*. Thermal shift assay indicates that the hAsp415Glu mutant has an increased fluorescence signal at room temperature which indicates that it is has a changed secondary/tertiary structure composition in comparison to the wild-type enzyme. In contrast to this, the hAsp415Val variant starts at a similar level like the wild-type indicating that this mutation has a minor effect on the enzyme structure. The negative first derivatives show that both mutants seem to destabilize the protein because both have a decreased melting temperature in comparison to the wild-type enzyme. (*C*) *Structural explanation for different effects of hALOX15 Asp415 mutants*. To explain the molecular effects of different mutants at the hAsp415 position, the corresponding residue rAsp416 was mutated *in silico* in the rabbit ALOX15 structure (PDB: 2P0M) and the energetically minimized (see Material and methods). The representation is the same as described in Fig. 3. The mutated residues are shown as white sticks and the resulting sterical clash which is caused by some mutations is shown as red dots. The rAsp416Glu mutation causes some sterical clash in the surrounding which might be the reason for the partial misfold whereas the rAsp416Val mutant almost cause no clash which fits well with practical observations in the thermal shift assay.

ALOX15B (Homo sapiens)	TRYTLHINTLARELLIVPGQVVDRSTGIGIEGFSELIQRNM	446
ALOX15B (Rattus norvegicus)	TRYTLHINTLARELLIAPGKVVDKSTGLGIGGFSDLIKRNM	447
ALOX15B (Mus musculus)	IRYTLHINTLARELLVAPGKLIDKSTGLGTGGFSDLIKRNM	447
ALOXE3 (Rattus norvegicus)	TRYTLQVNTIARATLLNPDGLVDKVTSIGRRGLIYLMSTGL	481
ALOXE3 (Mus musculus)	TRYTLQVNTIARATLLNPDGLVDKVTSIGRQGLIYLMSTGL	481
ALOXE3 (Homo sapiens)	TRYTLQVNTIARATLLNPEGLVDQVTSIGRQGLIYLMSTGL	481
ALOX12B (Bos taurus)	TRYTIQINSIGRAVLLNEGGLSARSMSLGLAGFAEAMVRAL	469
ALOX12B (Homo sapiens)	TRYTVQINSIGRAVLLNEGGLSAKGMSLGVEGFAGVMVRAL	471
ALOX12B (Mus musculus)	TRYNVQINSIGRALLLNKGGLSARAMSLGLEGFAQVMVRGL	471
ALOX12B (Rattus norvegicus)	TRYNVQINSIGRALLLNKGGLSARAMSLGLEGFAQVMVRGL	471
ALOX12B (Xenopus laevis)	LRYTLEINTLARQTLIGPDGFFDQAVVIGNGGVPVLLARAT	440
ALOX12B (Xenopus tropicalis)	LRYTLEINTLARQTLIGPKGLFDQAVVTGNGGVPVLLARAM	439
ALOX5 (Mus musculus)	VRFTIAINTKAREQLICEYGLFDKANATGGGGHVQMVQRAV	441
ALOX5 (Rattus norvegicus)	VRFTIAINTKAREQLNCEYGLFDKANATGGGGHVQMVQRAV	440
ALOX5 (Homo sapiens)	VRFTIAINTKAREQLICECGLFDKANATGGGGHVQMVQRAM	441
ALOX5 (Bos taurus)	VRFTIAINTKAREQLICEYGLFDKANATGGGGHVQMVQRAM	441
ALOX5 (Canis lupus fam.).	VRFTIAINTKAREQLICEYGLFDKANATGGGGHVQMVQRAM	443
ALOX5 (Danio rerio)	IRFTIAINTKAREQLICECGLFDKANGTGGGGHIELVQRSM	441
ALOX15 (Pongo abelii)	LRYTLEINVRARTGLVSDMGIFDQIMSTGGGGHVQLLKQAG	433
ALOX15 (Homo sapiens)	LRYTLEINVRARTGLVSDMGIFDQIMSTGGGGHVQLLKQAG	433
ALOX15 (Macaca mulatta)	LRYTLEINVRARTGLVSDMGVFDQVVSTGGGGHVELLRRAG	433
ALOX15 (Oryctolagus cuniculus)	LRYTLEINVRARNGLVSDFGIFDQIMSTGGGGHVQLLQQAG	434
ALOX15 (Mus musculus)	LLYTMEINVRARSDLISERGFFDKVMSTGGGGHLDLLKQAG	434
ALOX12 (Homo sapiens)	IRYTMEINTRARTQLISDGGIFDKAVSTGGGGHVQLLRRAA	433
ALOX12 (Bos taurus)	IRYTMEINTRARTQLISDGGIFDKAVSTGGGGHVHLLRRAL	433
ALOX12 (Mus musculus)	IRYTMEINTRSRTQLISDGGIFDQVVSTGGGGHVQLLTRAV	433

Fig. 6. Sequence alignment of different mammalian lipoxygenases. The figure shows an extract of a multiple amino acid sequence alignment of different mammalian lipoxygenases. The two putative interaction partners are shown in red whereas the position specificity determinants (Sloane) are shown in blue. They are well-conserved throughout the leukocyte-type (ALOX5, ALOX12 and ALOX15) lipoxygenases, but not throughout the epidermal lipoxygenases (ALOX12B, ALOX15B and ALOXE3).

site residues. The reduced catalytic activity and partial misfolding of the various hGly422 mutants might be explained by a sterical clash with other amino acids in the immediate surrounding. As glycine is the smallest possible amino acid, its substitution with more bulky residues at this position might be expected to induce side chain rearrangements of neighboring residues (Fig. 4C). Surprisingly, introduction of Arg (hGly422Arg) did not induce major structural rearrangement (Fig. 4C) and only a 50–60% reduction of the catalytic activity was observed. The structural basis for these observations has not been clarified. One might assume that the positively charged guanidine side chain forms a salt bridge with neighboring amino acids to stabilize the flexible loop region; however, in silico mutagenesis experiments did not confirm this hypothesis.

Although our activity data and the structural characterization of the recombinant enzyme variants suggest that most of mutations at hGly422 are deleterious for the enzyme and lead to protein misfolding

we cannot conclude the precise structural reason for this finding. Direct comparison of X-ray data obtained for hALOX15 wild-type and mutants would clearly be helpful to answer such questions. Unfortunately, despite multiple efforts to crystallize the two enzyme species, we were not able to generate high quality crystals suitable for X-ray analysis. The reason for this remains unclear, but the high degree of structural flexibility of this particular LOX isoform and its tendency for protein aggregation during the crystallization process might be discussed.

4.3. The functional glycine is conserved in other LOX isoforms

As indicated in Fig. 6 Gly422 of hALOX15 is conserved in many ALOX5, ALOX12 and ALOX15 isoforms of different species, but not in the epidermal LOXs (ALOX15B, ALOX12B, and ALOXE3) what suggests a functional role of this residue also in hALOX5 and hALOX12. Our activity

Table 4
Relative catalytic activities and product specificities of different hALOX5 and hALOX12 variants.
Recombinant expression of hALOX12 and product HPLC analysis was performed with crude cell lysate of 5 ml bacterial cultures (n = 5–10 bacterial clones for each mutant). For the hALOX5 aliquots of the Co-Sepharose elution fractions containing equal amounts of LOX protein as determined by western blot analysis were used for activity assays (n = 4). The amounts of HETE isomers were analyzed for each sample by HPLC and were used to measure the catalytic activity of different enzyme species. The HETE formation of the wild-type was set to 100%.

hALOX species	Share of 8-HETE %	Share of 12-HETE %	Share of 5-HETE %	Rel. activity % (AA)
hALOX12				
Wild-type	–	>99	–	100 ± 33
Gly422Glu	–	>99	–	30 ± 8
hALOX5				
Wild-type	12 ± 4	12 ± 4	76 ± 4	100 ± 3
Gly429Glu	48 ± 3	52 ± 3	4 ± 3	53 ± 5

assays with the Gly429Glu mutant of hALOX5 and Gly422Glu mutant of hALOX12 (Table 3) are consistent with this hypothesis. In addition, we found that the positional specificity of hALOX5 mutant upon Gly429Glu exchange is almost completely switched in favor of 8S- and 12R-H(p) ETE formation. Although, the molecular basis for the switch in positional specificity has not been explored Gly429 is located in close proximity to the position specificity determinants (Phe359, Ala424, Asn425, and Ile 603) of mammalian ALOX5 [33,40] and, thus, may contribute not only to the protein folding, but also to the fatty acid alignment at the active site. To prove this hypothesis additional mutagenesis experiments in connection with structural modeling and crystal trials of mutant enzyme-substrate complexes are required.

The model of hALOX15B reveals also a possibility for a polar interaction between Ile435 (Gly422 in hALOX15) and Asp428 (Asp415 in hALOX15) [41] (see Supporting information S3). On the other hand, ALOX15B does not follow the triad concept so that different way of substrate binding at the active site and the mode of its conversion may be predicted. In this context, Asp428–Ile435 interaction might be expected to have only minor functional importance in the case of hALOX15B. Nevertheless, Ile435 is located in the close proximity to the ALOX15B position specificity determinants identified by Jisaka et al. (Asp603 and Val604) [42,43], therefore functional importance of this should be explored by future experiments.

Mutagenesis studies with purified rabbit ALOX15 enzyme showed that the Gly-to-Glu exchange (rGly423Glu) causes reduction of the enzymatic activity and shifts the thermal denaturation parameters suggesting that structural alterations in the case of rabbit enzyme may be somewhat similar to those observed for human ALOX15 enzyme (see Supporting information S5).

4.4. Protein misfolding and aggregation has been implicated of pathological importance

We have shown that the reduced activity of the naturally occurring variant hALOX15 Gly422Glu is caused by a differential folding of the enzyme. Although the process of protein folding has been studied for several decades it still remains elusive how exactly it proceeds [44,45]. The pathophysiological role of misfolded proteins especially in neurodegenerative diseases has been discussed for years [46,47]. Here misfolded proteins form intra- and extracellular high molecular weight complexes, which are resistant toward proteolytic breakdown and exhibit neurotoxicity. More recently, protein misfolding was also suggested to be a reason for metabolic disorders such as short chain acyl-CoA dehydrogenase deficiency (SCAD), an inborn error of the mitochondrial fatty acid metabolism [48,49]. The lack of functional SCA impairs the energy metabolism of the allele carriers, which is the reason for patients' lethargy and hypoglycaemia [48,49]. In Spondyloepiphyseal dysplasia tarda (SEDT), a genetic disease characterized by impaired bone growth, misfolding of the SEDL (TRAPPC2) gene induces impaired cell differentiation and bone cell development [50]. The biological effect of misfolded hALOX15 variants (Thr560Met and Gly422Glu) in the cell still remains unclear. It might be possible that such misfolding reduces the biosynthesis of atheroprotective eicosanoids.

Acknowledgement

Appendix A. Supplementary data

Supplementary data to this article can be found online at http://dx.doi.org/10.1016/j.bbalip.2013.08.004.

References

[1] J.Z. Haeggström, C.D. Funk, Lipoxygenase and leukotriene pathways: biochemistry, biology, and roles in disease, Chem. Rev. 111 (2011) 5866–5898.

[2] I. Ivanov, D. Heydeck, K. Hofheinz, J. Roffeis, V.B. O'Donnell, H. Kuhn, M. Walther M, Molecular enzymology of lipoxygenases, Arch. Biochem. Biophys. 503 (2010) 161–174.

[3] A. Liavonchanka, I. Feussner, Lipoxygenases: occurrence, functions and catalysis, J. Plant Physiol. 163 (2006) 348–357.

[4] E.H. Oliw, Plant and fungal lipoxygenases, Prostaglandins Other Lipid Mediat. 68–69 (2002) 313–323.

[5] H. Porta, M. Rocha-Sosa, Lipoxygenase in bacteria: a horizontal transfer event? Microbiology 147 (2001) 3199–3200.

[6] R.E. Vance, S. Hong, K. Gronert, C.N. Serhan, J.J. Mekalanos, The opportunistic pathogen Pseudomonas aeruginosa carries a secretable arachidonate 15-lipoxygenase, Proc. Natl. Acad. Sci. U. S. A. 101 (2004) 2135–2139.

[7] J. Choi, J.K. Chon, S. Kim, W. Shin, Conformational flexibility in mammalian 15S-lipoxygenase: reinterpretation of the crystallographic data, Proteins 70 (2008) 1023–1032.

[8] N.C. Gilbert, S.G. Bartlett, M.T. Waight, D.B. Neau, W.E. Boeglin, A.R. Brash, M.E. Newcomer, The structure of human 5-lipoxygenase, Science 331 (2011) 217–219.

[9] S. Xu, T.C. Mueser, L.J. Marnett, M.O. Jr., Funk, crystal structure of 12-lipoxygenase catalytic-domain–inhibitor complex identifies a substrate-binding channel for catalysis, Structure 20 (2012) 1490–1497.

[10] S.A. Gillmor, A. Villaseñor, R. Fletterick, E. Sigal, M.F. Browner, The structure of mammalian 15-lipoxygenase reveals similarity to the lipases and the determinants of substrate specificity, Nat. Struct. Biol. 4 (1997) 1003–1009.

[11] M. Hersberger, Potential role of the lipoxygenase derived lipid mediators in atherosclerosis: leukotrienes, lipoxins and resolvins, Clin. Chem. Lab. Med. 48 (2010) 1063–1073.

[12] J. Wittwer, M. Hersberger, The two faces of the 15-lipoxygenase in atherosclerosis, Prostaglandins Leukot. Essent. Fatty. Acids 77 (2007) 67–77.

[13] D. Zhu, Y. Ran, Role of 15-lipoxygenase/15-hydroxyeicosatetraenoic acid in hypoxia-induced pulmonary hypertension, J. Physiol. Sci. 62 (2012) 163–172.

[14] L. Zhao, C.D. Funk, Lipoxygenase pathways in atherogenesis, Trends Cardiovasc. Med. 14 (2004) 191–195.

[15] H. Manev, H. Chen, S. Dzitoyeva, R. Manev, Cyclooxygenases and 5-lipoxygenase in Alzheimer's disease, Prog. Neuropsychopharmacol Biol. Psychiatry 35 (2011) 315–319.

[16] Y. Takahashi, H. Zhu, T. Yoshimoto, Essential roles of lipoxygenases in LDL oxidation and development of atherosclerosis, Antioxid. Redox Signal. 73 (2005) 425–431.

[17] D. Resnick, J.E. Chatterton, K. Schwartz, H. Slayter, M. Krieger, Structures of class A macrophage scavenger receptors. Electron microscopic study of flexible, multidomain, fibrous proteins and determination of the disulfide bond pattern of the scavenger receptor cysteine-rich domain, J. Biol. Chem. 271 (1996) 26924–26930.

[18] S. Ylä-Herttuala, M.E. Rosenfeld, S. Parthasarathy, C.K. Glass, E. Sigal, J.L. Witztum, D. Steinberg, Colocalization of 15-lipoxygenase mRNA and protein with epitopes of oxidized low density lipoprotein in macrophage-rich areas of atherosclerotic lesions, Proc. Natl. Acad. Sci. U. S. A. 87 (1990) 6959–6963.

[19] T. Takano, C. Mineo, Atherosclerosis and molecular pathology: mechanisms of cholesteryl ester accumulation in foam cells and extracellular space of atherosclerotic lesions, J. Pharmacobiodyn. 13 (1990) 385–413.

[20] A. Umar, Is 15-LOX-1 a tumor suppressor? Effects of gut-targeted 15-LOX-1 transgene expression on colonic tumorigenesis in mice, J. Natl. Cancer Inst. 104 (2012) 645–647.

[21] N.B. Janakiram, A. Mohammed, C.V. Rao, Role of lipoxins, resolvins, and other bioactive lipids in colon and pancreatic cancer, Cancer Metastasis Rev. 30 (2011) 507–523.

[22] C.N. Serhan, S. Yacoubian, R. Yang, Anti-inflammatory and proresolving lipid mediators, Annu. Rev. Pathol. 3 (2008) 279–312.

[23] C.N. Serhan, N. Chiang, T.E. Van Dyke, Resolving inflammation: dual anti-inflammatory and pro-resolution lipid mediators, Nat. Rev. Immunol. 8 (2008) 349–361.

[24] J. Zhao, Z. He, S. Ma, L. Li, Association of ALOX15 gene polymorphism with ischemic stroke in Northern Chinese Han population, J. Mol. Neurosci. 47 (2012) 458–464.

[25] K. Zhang, Y.Y. Wang, Q.J. Liu, H. Wang, F.F. Liu, Z.Y. Ma, Y.Q. Gong, L. Li, Two single nucleotide polymorphisms in ALOX15 are associated with risk of coronary artery disease in a Chinese Han population, Hear. Vessel. 25 (2010) 368–373.

[26] T.L. Assimes, J.W. Knowles, J.R. Priest, A. Basu, A. Borchert, K.A. Volcik, M.L. Grove, H.K. Tabor, A. Southwick, R. Tabibiazar, S. Sidney, E. Boerwinkle, A.S. Go, C. Iribarren, M.A. Hlatky, S.P. Fortmann, R.M. Myers, H. Kuhn, N. Risch, T. Quertermous, A near null variant of 12/15-LOX encoded by a novel SNP in ALOX15 and the risk of coronary artery disease, Atherosclerosis 198 (2008) 136–144.

[27] M. Hersberger, M. Müller, J. Marti-Jaun, I.M. Heid, S. Coassin, T.F. Young, V. Waechter, C. Hengstenberg, C. Meisinger, A. Peters, W. König, S. Holmer, H. Schunkert, N. Klopp, F. Kronenberg, T. Illig, No association of two functional polymorphisms in human ALOX15 with myocardial infarction, Atherosclerosis 205 (1) (2009 Jul) 192–196.

[28] K. Schurmann, M. Anton, I. Ivanov, C. Richter, H. Kuhn, M. Walther, Molecular basis for the reduced catalytic activity of the naturally occurring T560M mutant of human 12/15-lipoxygenase that has been implicated in coronary artery disease, J. Biol. Chem. 286 (2011) 23920–23927.

[29] S. Borngräber, R.J. Kuban, M. Anton, H. Kühn, Phenylalanine 353 is a primary determinant for the positional specificity of mammalian 15-lipoxygenases, J. Mol. Biol. 264 (1996) 1145–1153.

[30] D.L. Sloane, R. Leung, J. Barnett, C.S. Craik, E. Sigal, Conversion of human 15-lipoxygenase to an efficient 12-lipoxygenase: the side-chain geometry of amino acids 417 and 418 determine positional specificity, Protein Eng. (1995) 275–282.

[31] D.L. Sloane, R. Leung, C.S. Craik, E. Sigal, A primary determinant for lipoxygenase positional specificity, Nature 354 (1991) 149–152.

[32] R. Vogel, C. Jansen, J. Roffeis, P. Reddanna, P. Forsell, H.E. Claesson, H. Kuhn, M. Walther, Applicability of the triad concept for the positional specificity of mammalian lipoxygenases, J. Biol. Chem. 285 (2010) 5369–5376.

[33] K. Hofheinz, K.R. Kakularam, S. Adel, M. Anton, A. Polymarasetty, P. Reddanna, H. Kuhn, T. Horn, Conversion of pro-inflammatory murine Alox5 into an anti-inflammatory 15S-lipoxygenating enzyme by multiple mutations of sequence determinants, Arch. Biochem. Biophys. 530 (2013) 40–47.

[34] A. Di Venere, T. Horn, S. Stehling, G. Mei, L. Masgrau, A. González-Lafont, H. Kühn, I. Ivanov, Role of Arg403 for thermostability and catalytic activity of rabbit 12/15-lipoxygenase, Biochim. Biophys. Acta 1831 (2013) 1079–1088.

[35] M. Cristea, K. Engström, C. Su, L. Hörnsten, E.H. Oliw, Expression of manganese lipoxygenase in *Pichia pastoris* and site-directed mutagenesis of putative metalligands, Arch. Biochem. Biophys. 434 (2005) 201–211.

[36] E. Sudharshan, A.G. Rao, Involvement of cysteine residues and domain interactions in the reversible unfolding of lipoxygenase-1, J. Biol. Chem. 274 (1999) 35351–35358.

[37] E.S. Courtenay, M.W. Capp, R.M. Saecker, M.T. Record Jr., Thermodynamic analysis of interactions between denaturants and protein surface exposed on unfolding: interpretation of urea and guanidinium chloride m-values and their correlation with changes in accessible surface area (ASA) using preferential interaction coefficients and the local-bulk domain model, Proteins (Suppl. 4) (2000) 72–85.

[38] G.A. Jeffrey, An Introduction to Hydrogen Bonding, Oxford University Press, 1997.

[39] 1000 Genomes Project Consortium, G.R. Abecasis, A. Auton, L.D. Brooks, M.A. DePristo, R.M. Durbin, R.E. Handsaker, H.M. Kang, G.T. Marth, G.A. McVean, 692 other co-workers, An integrated map of genetic variation from 1,092 human genomes, Nature 491 (2012) 56–65.

[40] K. Schwarz, M. Walther, M. Anton, C. Gerth, I. Feussner, H. Kuhn, Structural basis for lipoxygenase specificity. Conversion of the human leukocyte 5-lipoxygenase to a 15-lipoxygenating enzyme species by site-directed mutagenesis, J. Biol. Chem. 276 (2001) 773–779.

[41] N. Arora N, V.K. Singh, K. Shah, S. Pandey-Rai, Qualitative and quantitative analysis of 3D predicted arachidonate 15-lipoxygenase-B (15-LOX-2) from *Homo sapiens*, Bioinformation 8 (12) (2012) 555–561.

[42] M. Jisaka, R.B. Kim, W.E. Boeglin, A.R. Brash, Identification of amino acid determinants of the positional specificity of mouse 8S-lipoxygenase and human 15S-lipoxygenase-2, J. Biol. Chem. 275 (2000) 1287–1293.

[43] G. Coffa, A.R. Brash, A single active site residue directs oxygenation stereospecificity in lipoxygenases: stereocontrol is linked to the position of oxygenation, Proc. Natl. Acad. Sci. U. S. A. 101 (2004) 15579–15584.

[44] K.A. Dill, J.L. MacCallum, The protein-folding problem, 50 years on, Science 338 (2012) 1042–1046.

[45] K.A. Dill, S.B. Ozkan, M.S. Shell, T.R. Weikl, The protein folding problem, Annu. Rev. Biophys. 37 (2008) 289–316.

[46] T.K. Chaudhuri, S. Paul, Protein-misfolding diseases and chaperone-based therapeutic approaches, FEBS J. 273 (2006) 1331–1349.

[47] E.I. Agorogiannis, G.I. Agorogiannis, A. Papadimitriou, G.M. Hadjigeorgiou, Protein misfolding in neurodegenerative diseases, Neuropathol. Appl. Neurobiol. 30 (2004) 215–224.

[48] C.B. Pedersen, P. Bross, V.S. Winter, T.J. Corydon, L. Bolund, K. Bartlett, J. Vockley, N. Gregersen, Misfolding, degradation, and aggregation of variant proteins. The molecular pathogenesis of short chain acyl-CoA dehydrogenase (SCAD) deficiency, J. Biol. Chem. 278 (48) (Nov 28 2003) 47449–47458.

[49] J. Reena, M.J. Bennett, J. Vockley, Mini-Review: Short-Chain Acyl-Coenzyme A Dehydrogenase Deficiency, Mol. Genet. Metab. 95 (2008) 195–200.

[50] M.Y. Choi, C.C. Chan, D. Chan, K.D. Luk, K.S. Cheah, J.A. Tanner, Biochemical consequences of sedlin mutations that cause spondyloepiphyseal dysplasia tarda, Biochem. J. 423 (2009) 233–242.